

# Homo- and Cross-[2+2]-Cycloaddition of 1,1-Diphenylsilene and 1,1-Diphenylgermene. Absolute Rate Constants for Dimerization and the Molecular Structures and Photochemistry of the Resulting 1,3-Dimetallacyclobutanes

Nicholas P. Toltl, Mark Stradiotto, Tracy L. Morkin, and William J. Leigh\*

Department of Chemistry, McMaster University, 1280 Main Street West,  
Hamilton, Ontario, L8S 4M1 Canada

Received June 10, 1999

Absolute rate constants for the head-to-tail [2+2]-dimerization of 1,1-diphenylsilene and 1,1-diphenylgermene have been determined in hexane and isooctane solution at 23 °C by laser flash photolysis, using the corresponding 1,1-diphenylmetallacyclobutanes as precursors. This requires knowledge of the molar extinction coefficients at the UV absorption maxima of the two transient species, which have been determined by a transient actinometric procedure. The rate constants for dimerization of the two compounds are similar and within a factor of about 2 of the diffusional rate constant in both cases. The 1,3-dimetallacyclobutane dimerization products have been prepared by direct photolysis of the corresponding 1,1-diphenylmetallacyclobutanes in dry isooctane. In addition, 1,1,3,3-tetraphenyl-1-germa-3-silacyclobutane has been prepared by photolysis of a 1:1 mixture of the two metallacyclobutanes. The solid-state structures of the three 1,3-dimetallacyclobutanes have been determined by single-crystal X-ray crystallography, and their photochemistry has been studied. Laser flash and/or steady-state photolysis experiments indicate that all three compounds cyclorevert to the corresponding 1,1-diphenylmetallaenes upon photolysis in hydrocarbon solvents, most likely via the same ( $M-C-M'-C$ ) 1,4-biradical intermediates which link the metallaenes with their corresponding dimers via stepwise dimerization mechanism. The quantum yield for photocycloreversion of the digermacyclobutane is roughly one-fourth that of 1,1-diphenylgermacyclobutane. However, it is about 3 times higher than that for the silagermacyclobutane and roughly 15 times higher than that for the disilacyclobutane. Singlet lifetimes have been determined for the metallacyclobutanes and the disila- and digermacyclobutanes using single photon counting techniques. The implications of these results for the mechanisms of the head-to-tail [2+2]-dimerization of silenes and germenes are discussed.

## Introduction

The chemistry of multiple bonds between carbon and one of the heavier group 14 elements such as silicon or germanium has been of considerable interest over the past few decades.<sup>1–3</sup> The combined effects of a low  $\pi$ -bond energy and the differences in electronegativity between carbon and the heteroatom make such bonding situations unfavorable thermodynamically, and as a result, most known silenes and germenes exist only as transient species in the gas phase and in solution. Bimolecular reaction with oxygen-, nitrogen-, or even carbon-centered nucleophiles is virtually always relatively facile and occurs at rates in excess of ca.  $10^7 M^{-1} s^{-1}$  in derivatives bearing simple alkyl or aryl substituents at the double bond.<sup>4–6</sup> This reactivity is supplanted by self-reaction (i.e., dimerization) when nu-

cleophiles are carefully excluded. Of course, a number of "stable" derivatives are known in both cases, but to the extent that these compounds always contain one or more sterically bulky substituents at one or both sites of the  $M=C$  bond, their stability is often more a reflection of a kinetic persistence toward dimerization than to actual thermodynamic stabilization effects.

Head-to-tail [2+2]-cycloaddition to yield the corresponding 1,3-dimetallacyclobutane derivative is the most common mode of dimerization for both silenes and germenes, in keeping with the substantial natural polarity of the  $\delta^+M=C\delta^-$  bond.<sup>1,2</sup> The head-to-head regiochemistry is common with derivatives bearing sterically bulky substituents at carbon, particularly when they also reduce the natural  $M=C$  bond polarity through electronic effects. Silenes of this type show enhanced kinetic stability compared to naturally polar-

(1) Brook, A. G.; Brook, M. A. *Adv. Organomet. Chem.* **1996**, *39*, 71.

(2) Barrau, J.; Escudié, J.; Satgé, J. *Chem. Rev.* **1990**, *90*, 283.

(3) Escudié, J.; Couret, C.; Ranaivonjatovo, H.; Satgé, J. *Coord. Chem. Rev.* **1994**, *130*, 427.

(4) Leigh, W. J. *Pure Appl. Chem.* **1999**, *71*, 453.

(5) Leigh, W. J.; Kerst, C.; Boukherroub, R.; Morkin, T. L.; Jenkins, S.; Sung, K.; Tidwell, T. T. *J. Am. Chem. Soc.* **1999**, *121*, 4744.

(6) Leigh, W. J.; Boukherroub, R.; Kerst, C. *J. Am. Chem. Soc.* **1998**, *120*, 9504.

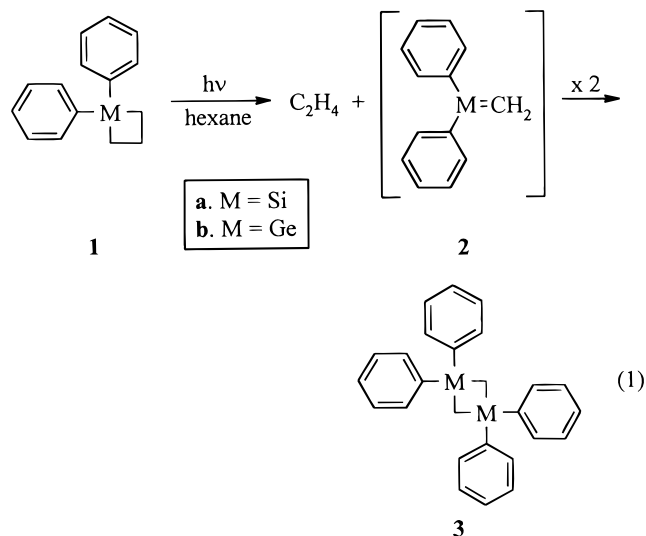
ized derivatives and often dimerize reversibly; when simple alkyl substituents are present at carbon, the main dimeric product is usually that corresponding to formal ene-addition rather than [2+2]-cycloaddition.

Until recently, the commonly accepted view was that the head-to-tail dimerization of silenes proceeds via a concerted  $\pi 2s + \pi 2s$  cycloaddition mechanism, in which the normal symmetry-imposed barrier for such a process is reduced due to the strong polarization of the C=Si bond. Head-to-head dimerization, on the other hand, is thought to proceed in stepwise fashion involving a  $\cdot\text{C}-\text{Si}-\text{Si}-\text{C}\cdot$  1,4-biradical intermediate resulting from initial Si-Si bond formation.<sup>7-9</sup> Recent high-level ab initio theoretical calculations have raised serious questions regarding the mechanism for the head-to-tail dimerization of naturally polarized silenes. Depending on the level of theory employed, the lowest energy pathway varies between concerted<sup>10</sup> and stepwise, the latter involving the initial formation of either an anti  $\cdot\text{Si}-\text{C}-\text{Si}-\text{C}\cdot$  biradical<sup>11,12</sup> or an anti  $\cdot\text{C}-\text{Si}-\text{Si}-\text{C}\cdot$  biradical, which undergoes concerted rearrangement to the head-to-tail dimer.<sup>13</sup> Much less is known about germene dimerization, although both head-to-tail and head-to-head dimers have been reported,<sup>2</sup> and the effects of substituents on the preferred regiochemistry appear to be the same as with silenes.<sup>14</sup> As far as we are aware, germene dimerization has not yet been examined computationally.

So far only one solution-phase kinetic study has been reported, on the head-to-head ene-type dimerization of a stabilized silene.<sup>15</sup> It is interesting to note that the reported Arrhenius parameters ( $E_a = 0.2 \pm 0.1$  kcal/mol and  $\log A = 7 \pm 1$ ) are indeed consistent with a stepwise reaction mechanism, involving some intermediate (a 1,4-biradical, for example) which partitions between product (via intramolecular disproportionation) and starting materials at similar rates. The gas-phase dimerization of the naturally polarized silene  $\text{Me}_2\text{Si}=\text{CH}_2$ , which is well-known to proceed in head-to-tail fashion,<sup>16</sup> is very rapid and also proceeds with a negligible Arrhenius activation energy over the 370–500 °C temperature range.<sup>17</sup> As has been recognized for some time,<sup>18</sup> such behavior is consistent with either concerted or stepwise reaction mechanisms.

We now wish to report the initial results of a detailed experimental study of the head-to-tail dimerization of "naturally polarized" silenes and germenes in solution, represented here by 1,1-diphenylsilene (**2a**) and its

germanium analogue **2b**. We have previously shown that these two transient compounds can be conveniently generated and detected by laser flash photolysis of the corresponding 1,1-diphenylmetallacyclobutanes **1**;<sup>4</sup> both decay with predominant second-order kinetics when generated in solution in the absence of nucleophiles, consistent with the fact that they are both known to dimerize to the corresponding 1,1,3,3-tetraphenyl-1,3-dimetallacyclobutanes (**3**) (eq 1).<sup>19-21</sup> In several previous



papers, we have studied the kinetics and mechanisms of the bimolecular reactions of these potent electrophiles with various nucleophilic trapping agents.<sup>21-26</sup> These studies suggest that germenes can generally be expected to show 10–1000 times lower reactivity than silenes of corresponding structure, at least in polar addition reactions in which the first step is attack of the nucleophile at the metal end of the M=C bond. In the present paper, we probe whether this generalization applies as well to [2+2]-dimerization, through the determination of absolute rate constants for the dimerization of **2a** and **2b** in hydrocarbon solution at ambient temperature.

We have also isolated and structurally characterized the 1,3-dimetallacyclobutane dimers of the silene and germene (**3a** and **3b**, respectively) and of the 1-german-3-silacyclobutane (**3c**) derived from cross-[2+2]-cycloaddition of **2a** and **2b** (eq 2). To our knowledge, this is the first reported example of a silene-germene cross-cycloaddition reaction, and we had hoped to provide some qualitative information on its rate relative to those of the dimerization reactions of these two substrates. The X-ray crystallographic study of the three 1,3-dimetallacyclobutanes was prompted by the fact that our original structural assignment of the 1,1-diphenylgermene dimer was based only on spectroscopic and analytical data,<sup>21</sup> which are not entirely unambiguous

(7) Guse'nikov, L. E.; Nametkin, N. S. *Chem. Rev.* **1979**, *79*, 529.

(8) Raabe, G.; Michl, J. *Chem. Rev.* **1985**, *85*, 419.

(9) Brook, A. G.; Baines, K. M. *Adv. Organomet. Chem.* **1986**, *25*, 1.

(10) Seidl, E. T.; Grev, R. S.; Schaefer, H. F., III. *J. Am. Chem. Soc.* **1992**, *114*, 3643.

(11) Bernardi, F.; Bottoni, A.; Olivucci, M.; Robb, M. A.; Venturini, A. *J. Am. Chem. Soc.* **1993**, *115*, 3322.

(12) Bernardi, F.; Bottoni, A.; Olivucci, M.; Venturini, A.; Robb, M. *J. Chem. Soc., Faraday Trans.* **1994**, *90*, 1617.

(13) Venturini, A.; Bernardi, F.; Olivucci, M.; Robb, M. A.; Rossi, A. *J. Am. Chem. Soc.* **1998**, *120*, 1912.

(14) Bravo-Zhivotovskii, D.; Zharov, I.; Kapon, M.; Apeloig, Y. *J. Chem. Soc., Chem. Commun.* **1995**, 1625.

(15) Zhang, S.; Conlin, R. T.; McGarry, P. F.; Scaiano, J. C. *Organometallics* **1992**, *11*, 2317.

(16) Guse'nikov, L. E.; Flowers, M. C. *J. Chem. Soc., Chem. Commun.* **1967**, 864.

(17) Brix, Th.; Arthur, N. L.; Potzinger, P. *J. Phys. Chem.* **1989**, *93*, 8193.

(18) Houk, K. N.; Rondan, N. G.; Mareda, J. *Tetrahedron* **1985**, *41*, 1555.

(19) Jutzli, P.; Langer, P. *J. Organomet. Chem.* **1980**, *202*, 401.

(20) Auner, N.; Grobe, J. *J. Organomet. Chem.* **1980**, *197*, 147.

(21) Tolft, N. P.; Leigh, W. J. *J. Am. Chem. Soc.* **1998**, *120*, 1172.

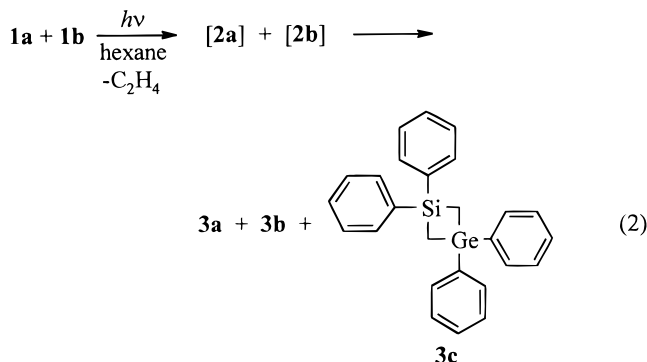
(22) Leigh, W. J.; Bradaric, C. J.; Sluggett, G. W. *J. Am. Chem. Soc.* **1993**, *115*, 5332.

(23) Leigh, W. J.; Bradaric, C. J.; Kerst, C.; Banisch, J. H. *Organometallics* **1996**, *15*, 2246.

(24) Bradaric, C. J.; Leigh, W. J. *J. Am. Chem. Soc.* **1996**, *118*, 8971.

(25) Bradaric, C. J.; Leigh, W. J. *Can. J. Chem.* **1997**, *75*, 1393.

(26) Bradaric, C. J.; Leigh, W. J. *Organometallics* **1998**, *17*, 645.



considering the symmetry possessed by both possible isomeric structures. The structure of the silene dimer **3a** was originally established on the basis of comparisons to an authentic sample made by an independent route,<sup>19,20</sup> but its crystal structure has evidently not been determined. We felt that it would be useful to do so, as it provides an opportunity to compare the absolute structures of a homologous series of 1,3-dimetallacyclobutanes which differ only in the identity of the ring heteroatoms.

Finally, we have studied the photochemistry of the three 1,3-dimetallacyclobutanes in some detail, with the intent of establishing their relative propensities toward [2+2]-cycloreversion to regenerate the silene and/or germene. The photolyses of these compounds provide a possible entry point to the potential energy surface corresponding to one of the nonconcerted (\*M–C–M–C• biradical) mechanisms for silene and germene [2+2]-dimerization, since there is good evidence to suggest, at least for 1,3-disilacyclobutanes, that photolysis results in initial Si–C bond cleavage to yield a 1,4-biradical intermediate.<sup>27,28</sup> Photolysis of **3a** in solution purportedly does *not* lead to cycloreversion,<sup>19</sup> but nothing appears to be known of the behavior of 1,3-silagermacyclobutanes or -digermacyclobutanes in this regard. Our results afford a few potentially relevant pieces of information on the mechanisms of silene and germene dimerization and allow a comparison of at least one aspect of the reactivity of 1,3-dimetallacyclobutane derivatives as a function of the heteroatom.

## Results and Discussion

**Homo- and Cross-[2+2]-Cycloaddition of 1,1-Diphenylsilene and 1,1-Diphenylgermene.** As has been reported previously,<sup>19–21</sup> steady-state photolysis of deoxygenated 0.01 M solutions of 1,1-diphenylsilacyclobutane (**1a**) or 1,1-diphenylgermacyclobutane (**1b**) in cyclohexane or cyclohexane-*d*<sub>12</sub> led in each case to the formation of a single major product. The two compounds were each isolated in analytically pure form by radial chromatography and identified as the 1,3-dimetallacyclobutanes **3a** and **3b**, respectively (eq 1).

The quantum yield for formation of 1,1-diphenylgermene (**2b**) from photolysis of **1b** was determined by merry-go-round photolysis of a deoxygenated 0.01 M solution of the germacyclobutane in cyclohexane con-

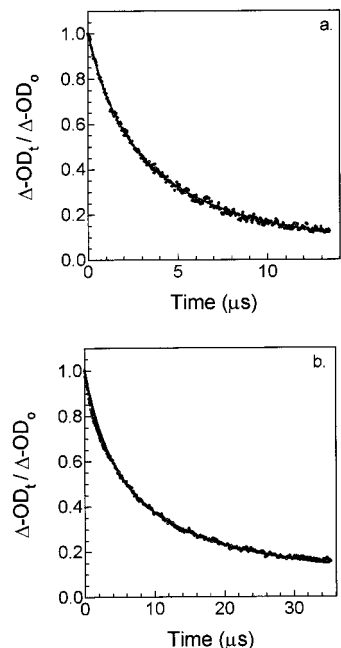


**Figure 1.** Transient decays for **2a** (a) and **2b** (b) in hexane at 23 °C. The solid lines represent the fit of the data to eqs 7 and 8, respectively.

taining 0.5 M methanol, which leads to quantitative trapping of the germene as methyldiphenylgermanium methoxide (**4b**).<sup>21</sup> The formation of methoxymethyldiphenylsilane (**4a**) from photolysis of 1,1-diphenylsilacyclobutane (**1a**) under the same conditions ( $\Phi_{4a} = 0.21 \pm 0.02$ <sup>23</sup>) was employed as actinometer. The photolyses were monitored at several conversions below ~10%, and the relative quantum yields for formation of **4a** and **4b** were taken as the relative slopes of product concentration versus time plots. The experiment afforded a value of  $\Phi_{4b} = 0.22 \pm 0.02$ .

Laser flash photolysis of continuously flowing, air- or nitrogen-saturated solutions of **1a** and **1b** in hexane or isooctane gave rise to the readily detectable transient absorptions which we have previously assigned to 1,1-diphenylsilene (**2a**) and 1,1-diphenylgermene (**2b**), respectively.<sup>4,21</sup> The decay of the germene followed strict second-order kinetics under these conditions, while the silene exhibited mixed second- and pseudo-first-order decay kinetics due to competing dimerization and reaction with traces of water in the solvent. Representative decay traces (in the form  $\Delta OD_t / \Delta OD_0$  vs time) are shown in Figure 1. The second-order rate coefficients ( $2k_{\text{dim}} / \epsilon_{325\text{-nm}}$ ) were obtained by nonlinear least-squares fitting of data from several experiments with each compound (see Experimental Section for details); the values measured in hexane were identical to those measured in isooctane within experimental error for both compounds, and so the averages were calculated using data from both solvents. The results are  $2k_{\text{dim}} / \epsilon_{325\text{-nm}} = (2.45 \pm 0.34) \times 10^6 \text{ cm s}^{-1}$  for **2a** (average of 4 determinations) and  $2k_{\text{dim}} / \epsilon_{325\text{-nm}} = (1.56 \pm 0.42) \times 10^6 \text{ cm s}^{-1}$  for **2b** (average of 7 determinations). The errors are quoted as the standard deviations from the mean values and correspond to confidence intervals of ~85% and ~95%, respectively.

Extinction coefficients ( $\epsilon$ ) were determined for **2a,b** in hexane solution at their absorption maxima (325 nm)

(27) Yoo, B. R.; Lee, M. E.; Jung, I. N. *Organometallics* **1992**, *11*, 1626.

(28) Jung, I. N.; Pae, D. H.; Yoo, B. R.; Lee, M. E.; Jones, P. R. *Organometallics* **1989**, *8*, 2017.

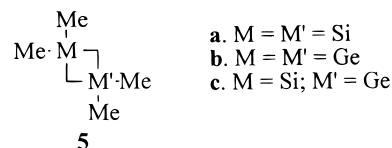
using the so-called intensity variation method.<sup>29,30</sup> This method involves comparing the  $\Delta OD$  value at the very beginning of the decay of the transient absorption ( $\Delta OD_0$ ) to the  $\Delta OD_0$  of an actinometer, whose photolysis yields a transient product of known  $\epsilon$  with a known quantum yield, as a function of excitation laser intensity. The actinometer employed was benzophenone, whose irradiation yields the triplet state ( $\lambda_{\max} = 525$  nm,  $\epsilon_{525-\text{nm}} = 6250 \pm 940 \text{ M}^{-1} \text{ cm}^{-1}$ )<sup>31</sup> with unit quantum yield. The substrate and actinometer solutions were optically matched at the laser wavelength (248 nm) to ensure equal light absorption, and the laser intensity was controlled using neutral density filters. Plots of  $\Delta OD_0$  versus laser intensity, examples of which are included as Supporting Information, were linear for all three compounds, although that for the actinometer showed some deviation at higher laser intensities (this is normal<sup>30</sup>). Extinction coefficients for **2a**, **b** at their absorption maxima were calculated from the relative slopes of the plots and the transient product quantum yields determined above. Duplicate determinations yielded average values of  $\epsilon_{325-\text{nm}} = 8900 \pm 1800 \text{ M}^{-1} \text{ cm}^{-1}$  for **2a** and  $\epsilon_{325-\text{nm}} = 11\,400 \pm 2700 \text{ M}^{-1} \text{ cm}^{-1}$  for **2b**. These values should be compared to that at the long-wavelength absorption maximum of 1,1-diphenylethylene,  $\epsilon_{250-\text{nm}} = 7680 \text{ M}^{-1} \text{ cm}^{-1}$ .<sup>32</sup>

Correction of the experimentally determined rate coefficients by these values affords estimates of  $k_{\text{dim}} = (1.1 \pm 0.3) \times 10^{10} \text{ M}^{-1} \text{ s}^{-1}$  and  $(9.0 \pm 3.2) \times 10^9 \text{ M}^{-1} \text{ s}^{-1}$  for the absolute rate constants for dimerization of **2a** and **2b**, respectively, in hexane/isooctane solution at 23 °C. The results indicate that in both cases dimerization is the most rapid reaction that these species undergo. Most importantly, the data indicate that the two species dimerize at essentially equal rates in hydrocarbon solvents and within a factor of about 2 of the diffusional limit. This is in sharp contrast to their relative reactivities toward nucleophiles such as amines, alcohols, ketones, or carboxylic acids, where the germene is 10–1000 times less reactive than the silene under similar conditions.<sup>4</sup> This presumably indicates that dimerization is substantially more exothermic than addition of oxygen- or nitrogen-centered nucleophiles in the case of the germene. These differences are almost certainly less pronounced in the case of the silene,<sup>33,34</sup> in agreement with the much reduced spread in the absolute rate constants for reaction of **2a** with itself and the various nucleophiles listed above.

With the indication that both **2a** and **2b** dimerize at close to the diffusion-controlled rate in solution at ambient temperatures, it seemed very likely that they would also undergo cross-cycloaddition if they could be generated together in the absence of nucleophiles. We were encouraged to attempt such an experiment, since

such a procedure might prove to be useful for the synthesis of mixed 1,3-dimetallacyclobutanes, of which relatively few examples are known. A statistical distribution of homo- and cross-cycloaddition products is most reasonably expected considering the absolute rate constants, yet photolysis of an equimolar mixture of **1a** and **1b** (0.05 M each) in sodium-dried hexane solution afforded the three dimetallacyclobutanes in relative yields of **3a**:**3b**:**3c** = 1.0:4.8:2.1 at conversions less than ~15%. This changed continuously over the course of the photolysis to a value of 1.0:3.0:2.0 at ~40% conversion.

Isolation of **3c** was accomplished by reverse-phase high-performance liquid chromatography, and its structure could be established unambiguously on the basis of its mass ( $M^+ = 434$ ) and <sup>1</sup>H NMR and <sup>13</sup>C NMR spectra. The high-field portions of the <sup>1</sup>H and <sup>13</sup>C NMR spectra show single resonances at <sup>1</sup>H  $\delta$  1.35 and <sup>13</sup>C  $\delta$  3.85, respectively, consistent with the  $D_{2h}$  symmetry of the head-to-tail cycloadduct. The <sup>1</sup>H and <sup>13</sup>C chemical shifts are intermediate between those in the corresponding spectra of **3a** (<sup>1</sup>H  $\delta$  1.10 and <sup>13</sup>C  $\delta$  0.85) and **3b** (<sup>1</sup>H  $\delta$  1.62 and <sup>13</sup>C  $\delta$  7.71), a trend which supports our original structural assignment for the germene dimer **3b**. The same trend in proton chemical shifts exists for the set of 1,1,3,3-tetramethyl-1,3-dimetallacyclobutanes **5a** (<sup>1</sup>H  $\delta$  0.03),<sup>35</sup> **5b** (<sup>1</sup>H  $\delta$  0.64),<sup>36</sup> and **5c** (<sup>1</sup>H  $\delta$  0.23).<sup>36</sup>



- a. M = M' = Si  
 b. M = M' = Ge  
 c. M = Si; M' = Ge

The distribution of the three 1,3-dimetallacyclobutanes obtained in this experiment at low conversions (**3a**:**3b**:**3c**  $\approx$  1.0:4.8:2.1) indicates that photolysis of **1b** is roughly 3 times more efficient than that of **1a** under these conditions. This is supported by the observation that the disappearance of **1b** proceeded significantly faster than **1a** during the initial stages of the photolysis. We were initially surprised by this result, since the quantum yields for photolysis and the extinction coefficients of the two compounds at the excitation wavelength employed (254 nm) are the same. Photolysis of mixtures containing higher (equimolar) concentrations of **1a** and **1b** led to product distributions that were even more dramatically skewed in favor of **3b**; for example, a distribution of **3a**:**3b**:**3c**  $\approx$  1:10:2.5 was obtained upon photolysis of a hexane solution of **1a** (0.2 M) and **1b** (0.2 M) to ~25% conversion. These results suggest that there is a second mechanism for excitation of **1b** in addition to direct light absorption, which results in the relative steady-state concentrations of **3b** and **3a** being significantly greater than 1 during the early stages of the photolysis. This second mechanism can most likely be identified as singlet energy transfer, which would be expected to favor excitation of **1b** if this compound has a lower excited singlet state energy and/or longer excited singlet state lifetime than **1a**. Indeed, while the static UV absorption spectra of **1a** and **1b** are superimposable, the fluorescence emission spectrum of **1b** is broader and shifted to lower energies ( $\lambda_{\max}^{\text{F}} = 305$  nm; see Support-

(29) Carmichael, I.; Hug, G. L. In *CRC Handbook of Organic Photochemistry*, Vol. I; Scaiano, J. C., Ed. CRC Press: Boca Raton, 1989; pp 369–404.

(30) Wintgens, V.; Johnston, L. J.; Scaiano, J. C. *J. Am. Chem. Soc.* **1988**, *110*, 511.

(31) Carmichael, I.; Hug, G. L. *J. Phys. Chem. Ref. Data* **1986**, *15*, 1.

(32) *The Sadtler Standard Spectra, 6401UV*; Sadtler Research Laboratories, Inc., 1966.

(33) Walsh, R. *Acc. Chem. Res.* **1981**, *14*, 246.

(34) Walsh, R. In *The Chemistry of Organic Silicon Compounds*; Patai, S., Rappoport, Z., Eds.; John Wiley & Sons Ltd.: New York, 1989; pp 371–391.

(35) Seyferth, D.; Attridge, C. J. *J. Organomet. Chem.* **1970**, *21*, 103.

(36) Mironov, V. F.; Gar, T. K.; Mikhailiyants, S. A. *Dokl. Akad. Nauk SSSR* **1969**, *188*, 718.

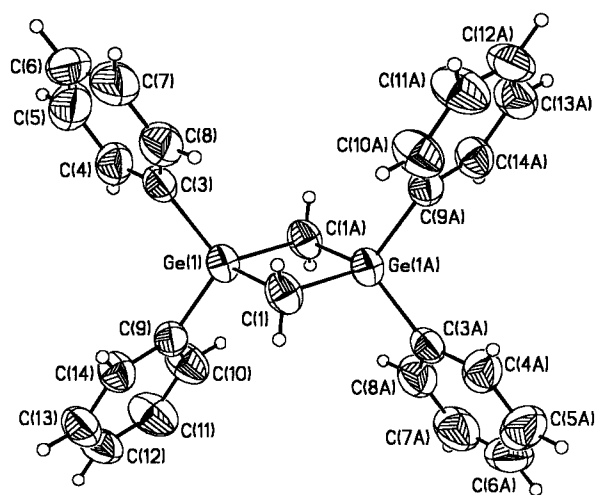
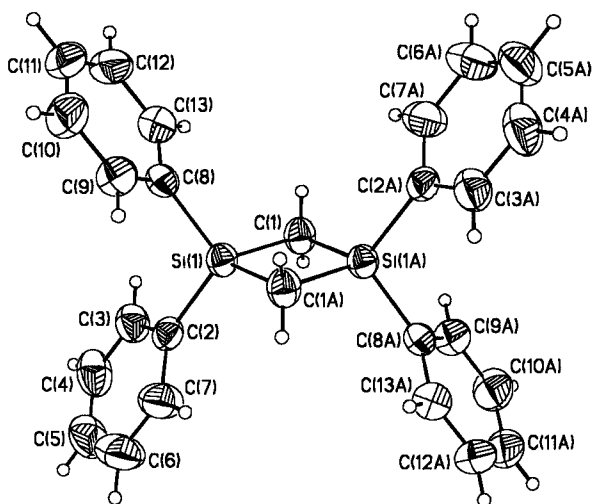


**Figure 2.** X-ray structures of **3a** (left) and **3b** (right), showing the atomic numbering schemes. Thermal ellipsoids are shown at the 50% probability level. For **3b**, only one of the two independent molecules is presented.

ing Information) compared to that of **1a** ( $\lambda_{\max}^F = 285$  nm),<sup>37</sup> indicating a significant difference in the geometries and energies of the relaxed excited singlet states of the two compounds.

Photolysis of solutions containing less than 0.05 M each of **1a, b** led to initial product distributions similar to those obtained in the 0.05 M experiments, but in these cases, the reaction mixtures also contained appreciable amounts of methyldiphenylsilanol and the corresponding disiloxane due to preferential trapping of **2a** by adventitious water in the solvent. The Si:Ge material balances in these experiments approached 1:1 as the concentration decreased however, indicating the expected falloff in singlet energy transfer processes with decreasing bulk substrate concentrations. Unfortunately, we were unable to dry the solvent to a sufficient level to allow a meaningful determination of the **3a:3b:3c** product distribution at low substrate concentrations; hence we are ultimately unable to estimate the relative rates of homo- versus cross-[2+2]-cycloaddition of **3a** and **3b** on the basis of these experiments.

In all of these experiments, the variation in the product distribution with increased photolysis times is partially due to the fact that the relative concentrations of the 1-metallacyclobutane starting materials (and hence the importance of singlet energy transfer processes) changes with photolysis time. A second contribution to this effect arises from the fact that the three products also undergo photocycloreversion to **2a** and/or **2b**, but with different efficiencies (vide infra). This results in equilibration of the three dimetallacyclobutanes at longer photolysis times, where the concentrations of the products are high enough to compete with the starting materials for light absorption.

**Molecular Structures of the 1,1,3,3-Tetraphenyl-1,3-dimetallacyclobutanes 3a–c.** The crystallographically determined structures of **3a, 3b**, and **3c** are shown in Figures 2 and 3, while the relevant refinement information and selected metrical parameters are collected in Tables 1–3. It is particularly interesting to note that no two of these structures are isomorphous, and very different symmetry relationships exist in the

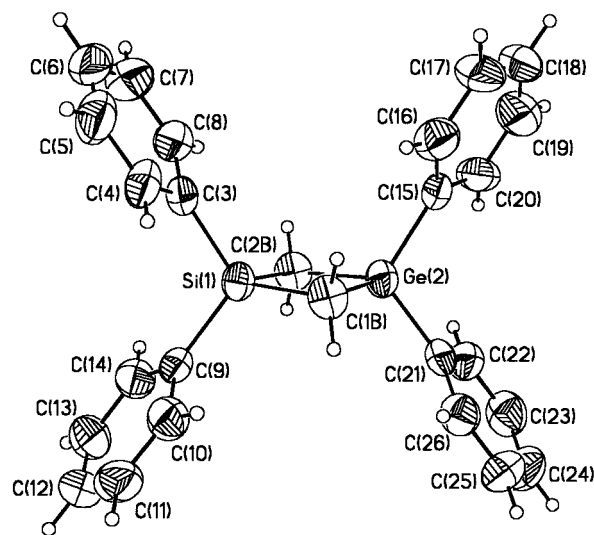


**Figure 3.** X-ray structure of **3c**, showing the atomic numbering scheme. Only the complete independent molecule is presented with thermal ellipsoids shown at the 50% probability level.

three lattice packings, despite the fact that only the identity of the heteroatoms differs in the three compounds.

The planar four-membered ring in **3a** (Figure 2, left) contains endocyclic angles of approximately 90°, comparable to those reported for other crystallographically characterized 1,3-disilacyclobutanes.<sup>38–42</sup> Perhaps surprisingly, these geometric constraints result in only a modest expansion of the associated exocyclic angles at the carbon and silicon tetrahedral centers, with no significant elongation of the Si–C ring bonds.<sup>43</sup> The transannular Si–Si distance (~2.62 Å) in **3a** is typical

(38) Braddock-Wilking, J.; Chiang, M. Y.; Gaspar, P. P. *Organometallics* **1993**, *12*, 197.

(39) Ishikawa, M.; Kovar, D.; Fuchikami, T.; Nishimura, K.; Kumada, M.; Higuchi, T.; Miyamoto, S. *J. Am. Chem. Soc.* **1981**, *103*, 2324.

(40) Boetze, B.; Herrschaft, B.; Auner, N. *Chem. Eur. J.* **1997**, *3*, 948.

(41) Auner, N.; Ziche, W.; Herdtweck, E. *J. Organomet. Chem.* **1992**, *426*, 1.

(42) Krempner, C.; Reinke, H.; Oehme, H. *Chem. Ber.* **1995**, *128*, 1083.

(43) Klebe, G. *J. Organomet. Chem.* **1985**, *293*, 147.

(37) Leigh, W. J.; Boukherroub, R.; Bradaric, C. J.; Cserti, C.; Schmeisser, J. M. *Can. J. Chem.* **1999**, *77*, 1136.

**Table 1. Crystallographic Collection and Refinement Parameters for 3a, 3b, and 3c**

	<b>3a</b>	<b>3b</b>	<b>3c</b>
empirical formula	C <sub>26</sub> H <sub>24</sub> Si <sub>2</sub>	C <sub>26</sub> H <sub>24</sub> Ge <sub>2</sub>	C <sub>26</sub> H <sub>24</sub> SiGe
molecular weight	392.63	481.63	437.13
description	colorless plate	colorless prism	colorless prism
cryst dimens, mm <sup>3</sup>	0.34 × 0.11 × 0.06	0.20 × 0.16 × 0.10	0.26 × 0.12 × 0.07
temp, K	300(2)	300(2)	300(2)
wavelength, Å	(Mo Kα) 0.71073	(Mo Kα) 0.71073	(Mo Kα) 0.71073
cryst syst	monoclinic	triclinic	triclinic
space group	C2/c	P(1)	P(1)
a, Å	20.5430(2)	10.2432(2)	6.1718(9)
b, Å	6.1256(2)	10.5455(1)	14.406(3)
c, Å	17.8378(3)	11.3542(1)	25.481(4)
α, deg.	90.000	103.452(1)	81.446(2)
β, deg.	97.206(1)	102.52(2)	85.695(3)
γ, deg.	90.000	93.074(1)	88.502(3)
volume, Å <sup>3</sup>	2226.95(8)	1157.42(3)	2233.7(6)
Z	4	2	4
calcd density, g/cm <sup>3</sup>	1.171	1.382	1.300
absorp coeff, mm <sup>-1</sup>	0.168	2.605	1.433
scan mode	ω-scans	ω-scans	ω-scans
F(000)	832	488	904
θ-range for collection, deg	2.00–22.49	1.90–22.50	1.43–22.50
index ranges	–26 ≤ h ≤ 26 –5 ≤ k ≤ 7 –23 ≤ l ≤ 23	–13 ≤ h ≤ 13 –13 ≤ k ≤ 13 –14 ≤ l ≤ 14	–6 ≤ h ≤ 6 –15 ≤ k ≤ 15 –27 ≤ l ≤ 27
no. of reflns collected	6265	8478	13941
no. of indep reflns	1461	2982	5856
R(int)	0.0511	0.0284	0.0708
no. of data/restraints/params	1456/0/135	2976/0/269	5856/0/523
goodness-of-fit on F <sup>2</sup>	1.033	1.037	0.843
final R indices (I > 2σ(I)) <sup>a</sup>	R1 = 0.0396; wR2 = 0.0916	R1 = 0.0290; wR2 = 0.0693	R1 = 0.0450; wR2 = 0.0751
R indices (all data) <sup>a</sup>	R1 = 0.0573; wR2 = 0.1012	R1 = 0.0370; wR2 = 0.0737	R1 = 0.1286; wR2 = 0.0937
transmission (max, min)	0.978, 0.453	0.704, 0.603	0.921, 0.681
largest diff peak, e/Å <sup>3</sup>	0.152	0.273	0.292
largest diff hole, e/Å <sup>3</sup>	–0.207	–0.237	–0.277

$$^a R1 = \sum(|F_o| - |F_c|)/\sum|F_o|; wR2 = [\sum(w(F_o^2 - F_c^2)^2)/\sum(w(F_o^2)^2)]^{0.5}.$$

**Table 2. Selected Bond Lengths (Å) and Angles (deg) for 3a and 3b**

Si(1)–Si(1a)	2.620(1)	Ge(1)–C(1a)	1.970(3)
Si(1)–C(1)	1.888(3)	Ge(1)–C(3)	1.954(3)
Si(1)–C(1a)	1.881(3)	Ge(1)–C(9)	1.945(3)
Si(1)–C(2)	1.876(2)	Ge(2)–C(2)	1.978(4)
Si(1)–C(8)	1.871(3)	Ge(2)–C(2a)	1.978(4)
C(1a)–Si(1)–C(1)	92.0(12)	Ge(2)–C(15)	1.949(3)
Si(1a)–C(1)–Si(1)	88.1(12)	Ge(2)–C(21)	1.945(4)
C(1)–Si(1)–C(2)	114.3(13)	C(1)–Ge(1)–C(1a)	90.9(2)
C(1)–Si(1)–C(8)	113.0(13)	C(2)–Ge(2)–C(2a)	90.0(2)
C(2)–Si(1)–C(8)	110.1(10)	Ge(1)–C(1)–Ge(1a)	89.1(2)
C(1a)–Si(1)–C(8)	112.7(13)	Ge(2)–C(2)–Ge(2a)	90.0(2)
C(1a)–Si(1)–C(2)	113.8(13)	C(3)–Ge(1)–C(9)	110.2(14)
Ge(1)–Ge(1a)	2.7704(6)	C(1a)–Ge(1)–C(3)	114.4(2)
Ge(2)–Ge(2a)	2.7980(7)	C(1)–Ge(1)–C(9)	112.8(2)
Ge(1)–C(1)	1.980(4)	C(1)–Ge(1)–C(3)	113.7(2)

for these systems and is consistent with a negligible bonding interaction between the silicon centers.<sup>44</sup>

The head-to-tail connectivity in **3b** (Figure 2, right) parallels that observed for **3a** and is in full agreement with the NMR and mass spectral data obtained for this compound.<sup>21</sup> Compounds **3a** and **3b** are not isomorphous, as evinced by the fact that **3b** crystallizes with two independent molecules per unit cell. As in the case of **3a**, both of the planar, square dimetallacyclic fragments in **3b** contain ring atoms possessing distorted tetrahedral geometries. The transannular Ge–Ge distances in both of the independent molecules of **3b** ( $d_{av}$

**Table 3. Selected Bond Lengths (Å) and Angles (deg) for 3c<sup>a,b</sup>**

M(1)–M(2)	2.694(1)	C(3)–M(1)–C(9)	110.1(2)
M(3)–M(3x)	2.689(2)	C(3)–M(1)–C(1A)	115.5(2)
M(4)–M(4x)	2.691(2)	C(9)–M(1)–C(1A)	112.8(2)
M(1)–C(1a)	1.909(5)	C(3)–M(1)–C(2A)	113.6(2)
M(1)–C(2a)	1.913(5)	C(9)–M(1)–C(2A)	112.5(2)
M(2)–C(1a)	1.924(5)	C(1A)–M(1)–C(2A)	91.3(2)
M(2)–C(2a)	1.935(5)	C(15)–M(2)–C(1A)	112.3(2)
M(3)–C(27)	1.912(6)	C(21)–M(2)–C(1A)	113.0(2)
M(3)–C(27a)	1.928(5)	C(15)–M(2)–C(2A)	114.6(2)
M(4)–C(40)	1.910(6)	C(21)–M(2)–C(2A)	114.9(2)
M(4)–C(40a)	1.912(6)	C(1A)–M(2)–C(2A)	90.2(2)

<sup>a</sup> The heavy atom positions of the complete independent molecule are denoted as M(1) and M(2), while the heavy atom positions of the two independent half-molecules are denoted as M(3) and M(4) (the corresponding symmetry-generated heavy atom positions are M(3x) and M(4x), respectively). <sup>b</sup> The refined occupancy of silicon at the heavy atom positions M(1) and M(2) are approximately 0.60 and 0.40, respectively (germanium contributing the remainder).

~2.78 Å) are similar to those previously reported in the literature for other 1,3-digermycyclobutane derivatives.<sup>45,46</sup>

Even though the structure of **3c** could be unambiguously assigned on the basis of NMR evidence (vide supra), it was also characterized by use of X-ray crystallography (Figure 3). To our knowledge, **3c** represents the first example of a crystallographically characterized

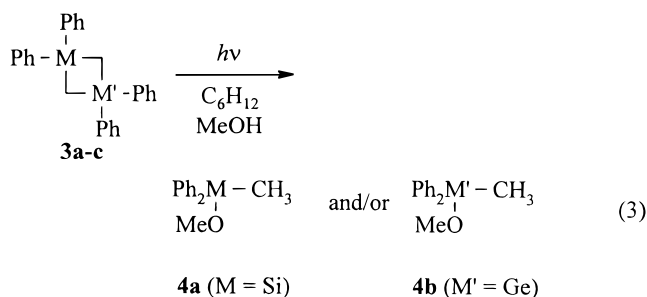
(45) Gusev, A. I.; Gar, T. K.; Los', M. G.; Alekseev, N. V. *J. Struct. Chem.* **1976**, *17*, 635.

(46) Zemlyanskii, N. N.; Borisova, I. V.; Bel'skii, V. K.; Kolosova, N. D.; Beletskaya, I. P. *Izv. Akad. Nauk SSSR, Ser. Khim.* **1983**, 869.

(44) Savin, A.; Flad, H.-J.; Flad, J.; Preuss, H.; von Schnering, H. *G. Angew. Chem., Int. Ed. Engl.* **1992**, *31*, 185.

molecule containing the 1-germa-3-silacyclobutane structure. Not unexpectedly, the data show a nearly statistical occupation disorder at the heavy atom sites in the three crystallographically independent molecules of **3c** present in the unit cell. However, the remainder of the structure is well-ordered and yields geometrical data that are consistent with an average of the related values in **3a** and **3b**. In **3c**, the average transannular silicon-germanium distance ( $\sim 2.69$  Å) agrees well with the corresponding average obtained from the related distances in **3a** and **3b** ( $d_{av} \sim 2.70$  Å), but is clearly outside of the range of a typical Si-Ge  $\sigma$ -bond ( $\sim 2.43$  Å).<sup>47,48</sup> Similarly, this disorder prevents the differentiation of unique Si-CH<sub>2</sub> and Ge-CH<sub>2</sub> bond lengths and instead leads to the observation of an M-CH<sub>2</sub> distance ( $\sim 1.92$  Å) that is close to the average of the Si-CH<sub>2</sub> ( $\sim 1.88$  Å) and Ge-CH<sub>2</sub> ( $\sim 1.98$  Å) distances found in **3a** and **3b**, respectively.

**Photochemistry of the 1,1,3,3-Tetraphenyl-1,3-dimetallacyclobutanes 3a-c.** Steady-state irradiation of deoxygenated solutions of **3a-c** in cyclohexane or cyclohexane-*d*<sub>12</sub> containing 0.5 M methanol led to the fairly clean formation of methoxymethyldiphenylsilane (**4a**) and/or methyldiphenylgermanium methoxide (**4b**), indicative of the formation of **2a** and/or **2b** as the initially formed products. Qualitatively, the photolysis of digermacyclobutane **3b** appeared to be roughly 3 times more efficient than that of **3c** and about 15 times more efficient than that of disilacyclobutane **3a**. The photolyses of **3b** and **3c** were clean, producing only the methoxysilane and/or -germane within the limits of our GC detection method. In the case of **3a**, on the other hand, the material balance was poor ( $\sim 10\%$ ), and GC/MS analysis indicated the coformation of 1,1'-bicyclohexyl in the early stages of the photolysis. This product is presumably derived from cyclohexyl radicals, further evidence of which was revealed by the additional formation of cyclohexanol and cyclohexanone in less completely deoxygenated solutions. These products are not formed in detectable yields in the photolyses of the other two compounds. It is not yet clear how cyclohexyl radicals are formed in this case, but their formation would be consistent with the involvement of a radical or biradical intermediate which is formed in higher steady-state concentrations in the photolysis of **3a** than in those of the other two compounds.



Quantum yields for formation of **4a/b** from photolysis of the three dimetallacyclobutanes were determined by

(47) Pannell, K. H.; Kapoor, R. N.; Raptis, R.; Parkanyi, L.; Fulop, V. J. *Organomet. Chem.* **1990**, *384*, 41.

(48) Suzuki, H.; Tanaka, K.; Yoshizoe, B.; Yamamoto, T.; Kenmotsu, N.; Matuura, S.; Akabane, T.; Watanabe, H.; Goto, M. *Organometallics* **1998**, *17*, 5091.

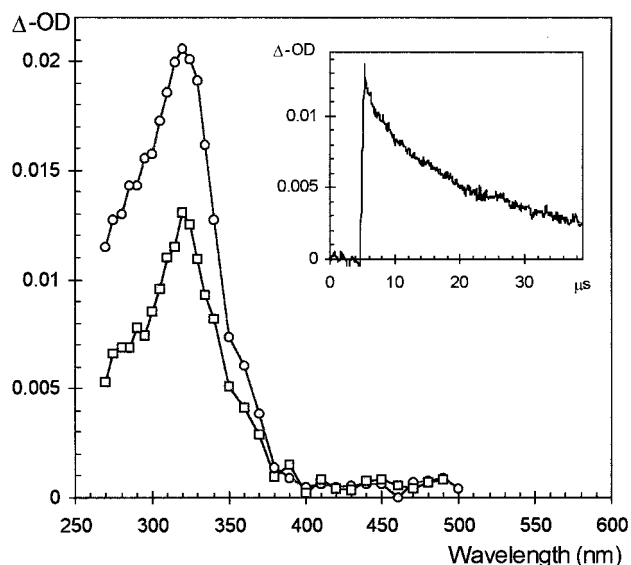


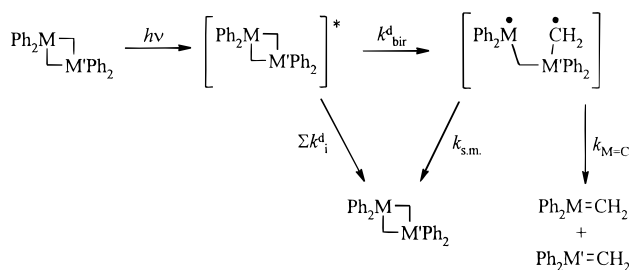
**Figure 4.** Transient absorption spectra recorded by 248-nm laser flash photolysis of optically matched, air-saturated hexane solutions of germacyclobutane **1b** (○) and digermacyclobutane **3b** (□), 0.1–1.0 μs after the laser pulse. The inset shows a representative decay trace for **3b**, recorded at the absorption maximum.

merry-go-round photolysis of deoxygenated 0.01 M solutions in cyclohexane containing 0.5 M methanol, using the procedure described above for **1b** (vide supra). These experiments afforded values of  $\Phi_{4a} = 0.007 \pm 0.003$  for the disilacyclobutane (**3a**),  $\Phi_{4a+4b} = 0.04 \pm 0.01$  for the germasilacyclobutane (**3c**), and  $\Phi_{4b} = 0.11 \pm 0.02$  for the digermacyclobutane (**3b**).

Similar indications of the relative reactivities of **3a** and **3b** toward photoinduced cycloreversion could be obtained by laser flash photolysis methods. Thus, 248-nm laser flash photolysis of a continuously flowing, air-saturated 0.0025 M solution of the digermacyclobutane in hexane gave rise to transient absorptions that were less intense but otherwise identical to those obtained from similar experiments with **1b**<sup>21</sup> and can thus be assigned to 1,1-diphenylgermane (**2b**). As was found with **1b**, saturation of the solution with nitrogen had no discernible effect on the spectrum or second-order decay kinetics of the transient. Figure 4 shows transient absorption spectra obtained from optically matched solutions of **3b** and **1b**, which illustrate both the similarities in the transient spectra obtained from the two compounds and the relative transient quantum yields. The intensity of the signal obtained from **3b** is roughly half that from **1b**, in good agreement with the relative quantum yields for formation of **2b** determined (as the methanol adduct **4b**) by steady-state photolysis of the two compounds in the presence of methanol.

Similar experiments with the disilacyclobutane (**3a**) did not yield detectable transient absorptions assignable to silene **2a**, not surprisingly in light of the quantum yield determined above by steady-state trapping methods. Interestingly, flash photolysis of this compound did yield a transient species whose formation and decay followed the laser pulse and which exhibited an absorption spectrum consisting of a single broad band centered at  $540 \pm 20$  nm. Though it is tempting to speculate that this species might be the 1,4-biradical derived from Si-CH<sub>2</sub> cleavage in **3a**, we have no evidence to support this

Scheme 1



assignment and hence must defer a full report of the transient spectroscopic behavior of this compound to a later date.

Assuming that photocycloreversion of the three dimetallacyclobutanes proceeds in all three cases by a stepwise mechanism involving a 1,4-biradical intermediate (**6**; see Scheme 1), then the overall quantum yield for formation of **2** ( $\Phi_{M=C}$ ) will be given by the product of two efficiency factors: that for biradical formation from the reactive excited state of the dimetallacyclobutane relative to other excited-state decay processes ( $\phi_{\text{bir}}$ ) and the efficiency with which the biradical cleaves to metallene relative to regenerating the starting material ( $\phi_{M=C}$ ; see eqs 4–6). While it is not possible to determine either of these state efficiencies independently in the present cases, it is most likely that variations in *both* contribute to the overall variation in  $\Phi_{M=C}$  throughout the series. One indication of the likely variation in the photophysical term ( $\phi_{\text{bir}}$ ) is provided by the fluorescence properties of **1a,b** and their dimetalla-counterparts **3a,b**.

$$\phi_{\text{bir}} = k_{\text{bir}} / (k_{\text{bir}} + \sum k_i^d) = k_{\text{bir}}^d \tau_s \quad (4)$$

$$\phi_{M=C} = k_{M=C} / (k_{M=C} + k_{s.m.}) \quad (5)$$

$$\Phi_{M=C} = \phi_{\text{bir}} \phi_{M=C} \quad (6)$$

Fluorescence emission spectra were measured for **3a,b** at 25 °C in argon-saturated isooctane solution and are shown in the Supporting Information along with those for **1a,b**. The spectra of the mono- and disilacyclobutane both show benzenoid emission bands centered at 285 nm. In the spectrum of **3a**, this is superimposed on a broad, less intense band at longer wavelengths, which might be ascribable to intramolecular excimer emission. Fluorescence lifetimes were determined by time-correlated single photon counting to be  $\tau = 2.6 \pm 0.1$  ns for **1a**, in good agreement with our previously reported value,<sup>37</sup> and  $\tau = 7.5 \pm 0.1$  ns for **3a**. Both decays fit acceptably to a single exponential, and lifetimes measured for **3a** at emission wavelengths of 290 and 325 nm did not differ within experimental error. In the case of **1a**, comparison of its singlet lifetime to that of dimethyldiphenylsilane suggests that Si–C bond cleavage in the lowest excited singlet state occurs at a comparable rate to those of the other processes that contribute to excited-state decay (fluorescence, internal conversion, etc.).<sup>37</sup> The significantly longer singlet lifetime observed for **3a** suggests that the second silicon atom slows this process down (hence reducing  $\phi_{\text{bir}}$ ), although the resulting (\*SiPh<sub>2</sub>CH<sub>2</sub>SiPh<sub>2</sub>CH<sub>2</sub>\*) 1,4-biradical might be expected to enjoy enhanced stabilization relative to the (\*SiPh<sub>2</sub>CH<sub>2</sub>CH<sub>2</sub>CH<sub>2</sub>\*) biradical de-

rived from **1a** due to  $\beta$ -silyl interactions.<sup>49</sup> One possible mechanism for such an effect is rapid equilibration of the reactive excited singlet state of **3a** with a much longer-lived, nonreactive (intramolecular) excimer state, the presence of which is suggested by the broad emission to the red of the benzenoid emission band in the fluorescence spectrum of this compound. This would also explain the similar fluorescence lifetimes measured for the two emitting species. Thus, we tentatively conclude that the substantially lower quantum yield for 1,1-diphenylsilene (**2a**) formation from photolysis of **3a** compared to that from **1a** is due to *both* a reduction in the partitioning of the excited singlet state between the corresponding 1,4-biradical (probably small, but certainly significant) and a reduction in the partitioning of the biradical between ring cleavage and coupling to regenerate the starting material. Thermodynamic factors dictate that the latter is likely to be quite large, since cycloreversion of **1a** yields **2a** + ethylene, while that of **3a** yields two molecules of **2a**.

We should also expect to find significant differences in the photophysical behavior of the mono- and digermacyclobutanes **1b** and **3b**. The fluorescence spectra of the two compounds suggest that indeed there are and, furthermore, that there are pronounced differences between the silicon and germanium homologues of both types of compound. In the case of the monometallacyclobutanes, the spectrum of the germanium compound is shifted to significantly lower energies than that of the silicon compound, indicating that a much larger change in geometry results from excitation of **1b** to its lowest excited singlet state than occurs with **1a**, whose fluorescence spectrum shows almost no Stokes shift whatsoever. The fluorescence decay of **1b** is more complex than that of **1a**, however; it analyses to two exponentials ( $\tau_1 = 3.0 \pm 0.2$  ns;  $\tau_2 = 12.8 \pm 0.1$  ns), which contribute almost equally to the overall decay. The emission properties of **3b** are even more difficult to interpret. The spectrum shows no similarity whatsoever to that of **1b**, and again, its decay consists of two components, although in this case there is clearly a major one which exhibits a lifetime  $\tau = 1.8 \pm 0.1$  ns. Unfortunately, this behavior makes it difficult to be completely confident of the reliability of our fluorescence data for the germanium compounds, although they (as well as those for **1a** and **3a**) were obtained from samples that were >99% pure (by GC), under conditions that led to <2% substrate photodecomposition during the course of the experiments. Thus, our data do not provide any really reliable clues as to how (\*MPh<sub>2</sub>CH<sub>2</sub>M'Ph<sub>2</sub>CH<sub>2</sub>\*) 1,4-biradical behavior might vary as a function of the heteroatom, a question which is of central importance in our attempts to ascertain the mechanisms of the head-to-tail dimerization of **2a** and **2b**.

## Summary and Conclusions

1,1-Diphenylsilene (**2a**) and 1,1-diphenylgermene (**2b**) undergo head-to-tail [2+2]-dimerization in hydrocarbon solution with absolute rate constants that are surprisingly similar to one another and are within a factor of  $\sim 2$  of the diffusional rate. The data suggest that in *both* cases the reaction proceeds with a very low activation

(49) Jarvie, A. W. P. *Organomet. Chem. Rev. A* **1970**, *6*, 153.

barrier, the magnitude of which cannot be significantly greater than the activation energy for diffusion in these solvents (ca. 2 kcal/mol). For **2a**, this agrees well with recent theoretical predictions for the dimerization of the parent molecule<sup>10–13</sup> and is consistent with a previous estimate of the Arrhenius activation energy for dimerization of 1,1-dimethylsilene in the gas phase.<sup>17</sup> Given the similarity in the rate constants for dimerization of **2a** and **2b**, it seems very likely that the dimerization of naturally polarized silenes and germenes proceeds by the same mechanism. Mechanistic commonalities have been documented previously in the reactions of **2a** and **2b** with nucleophilic reagents, although in these reactions the germene is generally much (10–1000 times) less reactive than the silene.<sup>4</sup>

The head-to-tail dimer of **2a**—disilacyclobutane **3a**—undergoes inefficient cycloreversion to the silene upon photolysis in solution in the presence of methanol. The quantum yield for photocycloreversion is 4–5 times lower than that of the homologous 1-sila-3-germacyclobutane (**3c**) and about 15 times lower than that of 1,3-digermacyclobutane **3b**. This variation in photo-reactivity is quite remarkable, considering that the monometallacyclobutanes **1a,b** cyclorevert with equal quantum efficiencies under similar conditions. These reactions most likely proceed via excited-state M–C bond cleavage to yield the corresponding  $\cdot\text{M}-\text{C}-\text{M}'-\text{C}\cdot$  biradical, which undergoes competing reclosure and fragmentation to the metallaene(s). They thus provide an entry point into the potential energy surface for nonconcerted silene/germene dimerization. Unfortunately however, the overall quantum yields for photocycloreversion ( $\Phi_{\text{M}=\text{C}}$ ) give an incomplete picture of the variation in biradical reactivity throughout the series. This is because  $\Phi_{\text{M}=\text{C}}$  is given by the product of two efficiency factors: that for biradical formation from the lowest excited singlet state ( $\phi_{\text{bit}}$ ) and that for cleavage of the biradical ( $\phi_{\text{M}=\text{C}}$ ). These efficiency factors cannot be extracted on the basis of the data we have available, and thus we are not yet able to rule out any of the three distinct mechanisms for the head-to-tail dimerization of silenes that have been previously suggested: concerted  $[\pi 2s + \pi 2s]$ -cycloaddition,<sup>10</sup> stepwise involving a  $\cdot\text{Si}-\text{C}-\text{Si}-\text{C}\cdot$  biradical,<sup>11,12</sup> or stepwise involving a  $\cdot\text{C}-\text{Si}-\text{Si}-\text{C}\cdot$  biradical.<sup>13</sup>

Future work in this area will be directed at defining the effects of temperature, solvent, and substituents on the absolute rate constants for dimerization of **1a** and **1b** in solution, as well as investigating in a more direct way the behavior of  $\cdot\text{M}-\text{C}-\text{M}-\text{C}\cdot$  biradicals as a function of the heteroatom.

### Experimental Section

<sup>1</sup>H and <sup>13</sup>C NMR spectra were recorded on Bruker AC200 or DRX500 NMR spectrometers in deuterated chloroform solution and are referenced to tetramethylsilane. Ultraviolet absorption spectra were recorded on Hewlett-Packard HP8451 or Perkin-Elmer Lambda 9 spectrometers. Low-resolution mass spectra and GC/MS analyses were determined using a Hewlett-Packard 5890 gas chromatograph equipped with a HP-5971A mass selective detector and a DB-5 fused silica capillary column (30 m × 0.25 mm; Chromatographic Specialties, Inc.). High-resolution desorption electron impact (DEI) mass spectra and exact masses were recorded on a VGH ZABE mass spectrometer. Exact masses employed a mass of 12.000000

for carbon. Infrared spectra were recorded on a BioRad FTS-40 FTIR spectrometer and are reported in wavenumbers. Fluorescence emission spectra and singlet lifetimes were determined on a Photon Technologies Inc. LS-100 spectrometer, which provides both steady-state and time-resolved (time-correlated single photon counting) capabilities. Samples for fluorescence experiments were contained in Suprasil quartz cuvettes, deoxygenated with a stream of dry argon, and sealed with Teflon tape.

Reverse phase HPLC separations were carried out using a Hewlett-Packard 1090 liquid chromatograph equipped with a built-in diode-array UV detector and a 5  $\mu\text{m}$  Vydac reversed phase column (25 cm × 4.6 mm i.d., Separations Group, Hesperia, CA). The HPLC was operated with a column temperature of 40 °C, a flow rate of 1.0 mL/min, and a monitoring wavelength range of 250–274 nm. The separation employed a gradient elution with water–acetonitrile mixtures (30% water → 81% water at 16 min → 90% water at 20 min). Under these conditions, ca. 1-mg samples of a mixture of the three dimetallacyclobutanes could be separated cleanly into the three components.

Analytical gas chromatographic analyses were carried out using a Hewlett-Packard 5890 gas chromatograph equipped with a flame ionization detector, a Hewlett-Packard 3396A recording integrator, conventional heated splitless injector, and a DB-1 fused silica capillary column (15 m × 0.20 mm; Chromatographic Specialties, Inc.). Semipreparative GC separations employed a Varian 3300 gas chromatograph equipped with a thermal conductivity detector and a 6 ft × 0.25 in. stainless steel OV-101 packed column (Chromatographic Specialties). Radial chromatographic separations employed a Chromatotron (Harrison Research, Inc.), 2- or 4-mm silica gel 60 thick-layer plates, and hexane/dichloromethane mixtures as eluant.

Acetonitrile (Caledon HPLC) was used as received from the supplier. Hexane and isooctane (BDH Omnisolv) were used as received or distilled from sodium. 1,1-Diphenylsilacyclobutane (**1b**) and 1,1-diphenylgermacyclobutane (**1b**) were prepared and purified as previously described.<sup>21,25</sup>

Preparative irradiations of **1a,b** employed a Rayonet Photochemical Reactor (Southern New England Ultraviolet Co.) equipped with 8–10 RPR-2537 lamps. Solutions of the metallocyclobutanes (0.25 g) were dissolved in hexane (15 mL), sealed in a quartz photolysis tube with a rubber septum, deoxygenated with dry argon, and irradiated to 20–50% conversion of starting material (6–10 h). The dimers (**3a,b**) were separated from residual starting material by radial chromatography and recrystallized from pentane. Their melting points (**3a**, mp 135–136 °C; **3b**, mp 120–121 °C) and spectroscopic data matched the previously reported data in both cases.<sup>19,21</sup> The following spectroscopic data for **3a** have not been reported previously: <sup>1</sup>H NMR,  $\delta$  = 1.10 (s, 4H), 7.31–7.36 (m, 12H), 7.50–7.56 (m, 8H); <sup>13</sup>C NMR,  $\delta$  = 0.85, 127.88, 129.42, 134.29, 137.37; IR (neat), 3065.7 (m), 3018.0 (m), 2999.5 (m), 2924.2 (m), 1428.0 (s), 1375.6 (m), 1344.4 (m), 1262.6 (m), 1110.4 (s), 1064.9 (s), 1024.7 (s), 936.6 (m); MS, *m/e* (I) = 392 (5), 377 (7), 314 (40), 301 (40), 257 (20), 237 (20), 223 (20), 181 (30), 157 (25), 105 (100), 91 (10), 79 (10); HRMS, calcd for C<sub>26</sub>H<sub>24</sub>Si<sub>2</sub>, 392.1408; found 392.1416.

**1,1,3,3-Tetraphenyl-(1-sila-3-germa)cyclobutane (3c)** was prepared by photolysis of a deoxygenated solution of **1a** (0.24 g, 1.07 mmol) and **1b** (0.27 g, 1.0 mmol) in hexane (20 mL), under conditions similar to those described above. The photolysis was stopped after ~40% conversion of the two starting materials, at which time capillary GC analysis indicated the mixture consisted of (in order of increasing retention time) **1a** (50%), **1b** (19%), **3a** (2.4%), **3c** (7.7%), and **3b** (6.4%). Radial chromatography of the crude reaction mixture after evaporation of the residual solvent allowed separation of **1a,b** from the three dimetallacyclobutanes, which eluted together and were hence isolated as a mixture. The

three compounds were successfully separated by reverse phase HPLC, after which **3c** was recrystallized from pentane to yield colorless prisms (mp 98–99 °C). The compound exhibited the following spectroscopic and analytical data: <sup>1</sup>H NMR,  $\delta$  = 1.31 (s, 4H), 7.31–7.36 (m, 12H), 7.46–7.51 (m, 4H), 7.52–7.59 (m, 4H); <sup>13</sup>C NMR,  $\delta$  = 3.75, 127.86, 128.22, 128.99, 129.37, 133.72, 134.19, 137.82, 138.97; IR (neat), 3070.2 (m), 2965.5 (m), 2858.3 (m), 1464.1 (m), 1425.8 (m), 1382.1 (m), 1259.1 (m), 1112.2 (s), 1069.8 (s), 1022.5 (s), 846.7 (w); MS,  $m/e$  (I) = 438 (5), 423 (5), 360 (35), 347 (50), 259 (100), 226 (10), 209 (10), 195 (15), 181 (15), 151 (15), 105 (20), 91 (10), 79 (5); HRMS, calcd for C<sub>26</sub>H<sub>24</sub>SiGe, 438.0834; found 438.0859.

Nanosecond laser flash photolysis experiments employed the pulses (248 nm; ca. 16 ns; 120–160 mJ) from a Lambda-Physik Compex 120 excimer laser filled with F<sub>2</sub>/Kr/He mixtures and a microcomputer-controlled detection system.<sup>21,50</sup> Solutions were prepared at concentrations such that the absorbance at the excitation wavelength (248 nm) was ca. 0.7 (2.5 × 10<sup>-3</sup> M) and were flowed continuously through a 3 × 7 mm Suprasil flow cell connected to a calibrated 100-mL reservoir.

Dimerization rate coefficients were calculated by nonlinear least-squares fitting of  $\Delta OD$  versus time data for **2a** using eq 7, the standard expression for mixed pseudo-first-order and second-order decay,<sup>51</sup> in which  $l$  is the path length (3 mm) and  $k_1$  is the pseudo-first-order component of the decay. The analyses afforded  $k_1$  values on the order of 10<sup>4</sup> s<sup>-1</sup>. The decay traces for **2b** were more predominantly second order, but plots of 1/( $\Delta OD$ )<sub>t</sub> versus time deviated significantly from linearity. Fitting the data to eq 7 gave statistically acceptable results, but  $k_1$  values were negative, i.e., characteristic of a pseudo-first-order *growth* to a relatively long-lived residual absorption. While the residual absorption is real, it is formed within the laser pulse, and hence the indication of a first-order growth can be considered an artifact.<sup>21</sup> Thus, the data were finally analyzed according to the more appropriate expression given in eq 8, where  $\Delta OD_{\infty}$  is the value of the residual absorption.  $\Delta OD_{\infty}$  did not exceed 10% of the initial signal intensity in any case, consistent with prior experience.<sup>21</sup>

$$(\Delta OD)_t / (\Delta OD)_0 = k_1 \exp(-k_1 t) / [k_1 + (2k_{\text{dim}}(\Delta OD)_0 / l \epsilon_{325\text{-nm}})(1 - \exp(-k_1 t))] \quad (7)$$

$$(\Delta OD)_t / (\Delta OD)_0 = (\Delta OD_{\infty}) / (\Delta OD)_0 + 1 / [1 + (2k_{\text{dim}}(\Delta OD)_0 / l \epsilon_{325\text{-nm}}) t] \quad (8)$$

**X-ray Crystallography.** Crystallographic data<sup>52</sup> for **3a**, **3b**, and **3c** were collected from suitable crystals which were grown from pentane and mounted on a glass fiber. The instrument used for the data collection was a P4 Siemens diffractometer equipped with a Siemens SMART 1K CCD area detector (using

the program SMART) and a rotating anode using graphite-monochromated Mo K $\alpha$  radiation ( $\lambda$  = 0.71073 Å). Data processing was carried out by use of the program SAINT, while the program SADABS was utilized for the scaling of diffraction data, the application of a decay correction, and an empirical absorption correction based on redundant reflections. The structures were solved by using the direct methods procedure in the Siemens SHELXTL program library and refined by full-matrix least-squares methods on  $F^2$  with anisotropic thermal parameters for all non-hydrogen atoms. Hydrogen atoms were added as fixed contributors at calculated positions, with isotropic thermal parameters based on the carbon atom to which they are bonded. In the crystal, **3a** is situated on a crystallographic inversion center, resulting in the observation of only half a molecule per asymmetric unit. A similar scenario exists for **3b**; however the asymmetric unit consists of two crystallographically independent half-molecules. For **3c**, the asymmetric unit was found to contain two half-molecules and one complete molecule, giving rise to a total of four molecules per unit cell. Given the asymmetry in the **3c** molecular framework, equal (50:50) occupancy of silicon and germanium in the heavy atom positions of the final refined structure for each of the two crystallographically independent half-molecules was assigned. However, when the distribution of silicon and germanium over the two heavy atom sites in the complete independent molecule was allowed to refine as a free variable (with the coordinates and thermal parameters of the disordered heavy atoms at each site constrained to refine to common values), an occupancy ratio of approximately 60:40 was found and subsequently utilized in the final refined model.

**Acknowledgment.** We thank D. Hughes for his assistance with high-resolution NMR spectra, the McMaster Regional Centre for Mass Spectrometry for high-resolution mass spectra and exact mass determinations, Professor Brian McCarty for his advice and assistance with chromatographic separations, and Professor Mark Steinmetz for helpful comments. The financial support of the Natural Sciences and Engineering Research Council (NSERC) of Canada is also gratefully acknowledged. M.S. and T.L.M. thank NSERC for postgraduate scholarships.

**Supporting Information Available:** Tables of atomic coordinates, bond lengths and angles, anisotropic displacement parameters, and hydrogen atom coordinates for **3a–c**, UV absorption and fluorescence emission spectra of **1a**, **1b** and **3a**, **3b**, and plots of  $\Delta OD_0$  versus laser intensity from flash photolysis of optically matched solutions of benzophenone, **1a** and **1b**, from which the extinction coefficients of **2a**, **2b** were calculated. This material is available free of charge via the Internet at <http://pubs.acs.org>.

OM990447K

(50) Leigh, W. J.; Workentin, M. S.; Andrew, D. J. *Photochem. Photobiol. A: Chem.* **1991**, *57*, 97.

(51) Espenson, J. H. *Chemical Kinetics and Reaction Mechanisms*, 2nd ed.; McGraw-Hill: New York, 1995.

(52) (a) SMART, Release 4.05; Siemens Energy and Automation Inc.: Madison, WI, 1996. (b) SAINT, Release 4.05; Siemens Energy And Automation Inc.: Madison, WI, 1996. (c) Sheldrick, G. M. SADABS (Siemens Area Detector Absorption Corrections); 1996. (d) Sheldrick, G. M. Siemens SHELXTL, Version 5.03; Siemens Crystallographic Research Systems: Madison, WI, 1994.